Membrane blebbing during apoptosis results from caspase-mediated activation of ROCK I

Mathew L. Coleman*†, Erik A. Sahai*†, Margaret Yeo*, Marta Bosch*, Ann Dewar‡ and Michael F. Olson*§

*CRC Centre for Cell and Molecular Biology, Chester Beatty Laboratories, The Institute of Cancer Research, 237 Fulham Road, London SW3 6JB, UK
‡National Heart and Lung Institute, Royal Brompton Hospital, Sydney Street, London SW3 6NP, UK.
†These authors contributed equally to this work
§e-mail: michael@icr.ac.uk

The execution phase of apoptosis is characterized by marked changes in cell morphology that include contraction and membrane blebbing. The actin–myosin system has been proposed to be the source of contractile force that drives bleb formation, although the biochemical pathway that promotes actin–myosin contractility during apoptosis has not been identified. Here we show that the Rho effector protein ROCK I, which contributes to phosphorylation of myosin light-chains, myosin ATPase activity and coupling of actin–myosin filaments to the plasma membrane, is cleaved during apoptosis to generate a truncated active form. The activity of ROCK proteins is both necessary and sufficient for formation of membrane blebs and for re-localization of fragmented DNA into blebs and apoptotic bodies.

The evolutionarily conserved execution phase of apoptosis is characterized by events that occur during the final stages of death, including cell contraction, dynamic membrane blebbing and DNA fragmentation. The distinct morphological transformation is one of the earliest described and most obvious aspects of apoptosis, but is also perhaps the least well characterized. Contractile force generated by actin–myosin cytoskeletal structures is thought to drive the formation of membrane blebs and apoptotic bodies[1–3], however, the biochemical pathway that promotes the generation of this force during apoptosis has not been identified.

The Rho GTPases (RhoA, B and C) are intracellular signalling molecules that regulate the actin cytoskeleton[4]. Upon activation, Rho proteins exchange GDP for GTP, transduce signals to downstream effector proteins and finally return to the inactive GDP-bound form by hydrolysing the bound GTP. Two isoforms of a serine/threonine kinase (Rho-associated kinases ROCK I and ROCK II) have been identified as effectors of Rho[5–7]. ROCK proteins bind to and are activated by GTP-bound Rho. Deletion of the carboxy-terminal region of ROCK activates the amino-terminal kinase domain both *in vitro* and *in vivo*[6,8–10]. Activation of ROCK proteins contributes positively to the stabilization of filamentous actin, phosphorylation of myosin light chains, myosin ATPase activity and coupling of actin–myosin filaments to the plasma membrane, leading to increased actin–myosin force generation and cell contractility[11–17].

As Rho and ROCK have been shown to contribute both to the formation of actin cytoskeletal structures and to consequent contractile force generation, we examined the role of this signalling pathway in the development of the apoptotic morphology. Here we show that the occurrence of apoptotic membrane blebbing is dependent on the function of ROCK but not on that of Rho. ROCK I, but not ROCK II, is cleaved during apoptosis by activated caspases, generating a truncated kinase with increased intrinsic activity. This cleaved form of the kinase is sufficient to drive cell contraction and membrane blebbing without caspase activation, which is consistent with a direct effect of ROCK-induced cell contractility on the generation of the apoptotic morphology. Finally, we show that ROCK activity and consequent membrane blebbing are required for redistribution of fragmented DNA from the nuclear region into membrane blebs and apoptotic bodies.

Results

ROCK activity is necessary for membrane blebbing. We created a cell-penetrating form of the *Clostridium botulinum* C3 toxin, which catalyses the specific ADP ribosylation and inactivation of Rho[18], by fusing a portion of the human immunodeficiency virus Tat-coding sequence to the N terminus of C3; we expressed and purified the resulting Tat–C3 toxin in *Escherichia coli*. We pretreated NIH 3T3 mouse fibroblasts with this toxin for 18 h and then subjected them to the apoptotic stimulus of 0.5 μM recombinant mouse tumour-necrosis factor-α (TNFα) plus 10 μg ml^{-1} cycloheximide (CHX). Although pretreatment with Tat–C3 was sufficient to modify all detectable RhoA and to block serum-stimulated formation of stress fibres (data not shown), Tat–C3 did not affect the generation of membrane blebs after treatment with TNFα, compared with cells treated with TNFα alone (Fig. 1a). In contrast, inhibition of ROCK activity using the small-molecule inhibitor Y-27632 (ref. 19) resulted in a marked reduction in formation of membrane blebs (Fig. 1a), although apoptotic cells still exhibited a rounded morphology compared with untreated cells. Expression of a dominant negative form of ROCK I[8] similarly reduced membrane blebbing during apoptosis (data not shown). Scanning electron microscopy of TNFα-treated cells revealed that, although the morphology of membrane blebs was altered by pretreatment with Tat–C3, the number of blebs was not significantly reduced (Fig. 1b). Cells treated with Y-27632, however, had very few large blebs and exhibited only small protrusions emanating from the cell surface (Fig. 1b). Consistent with the inability of Tat–C3 to inhibit blebbing, only a small and transient activation of RhoA was observed after treatment with TNFα plus CHX in a pull-down assay using the Rho-binding domain from the Rho effector Rhotekin[20,21] (Fig. 1c).

Activation of ROCK I by caspase-mediated cleavage. During apoptosis, a class of cysteine proteases called caspases act as effectors of the cell-death programme[22]. One mechanism by which caspases promote apoptosis is through cleavage and subsequent activation of protein kinases[23]. Western blotting of whole-cell lysates prepared from untreated or TNFα/CHX-treated NIH 3T3 cells showed no detectable cleavage of ROCK II (Fig. 2a) but significant cleavage of ROCK I, as well as cleavage of the well characterized caspase substrate poly-ADP ribose polymerase (PARP) after treatment with

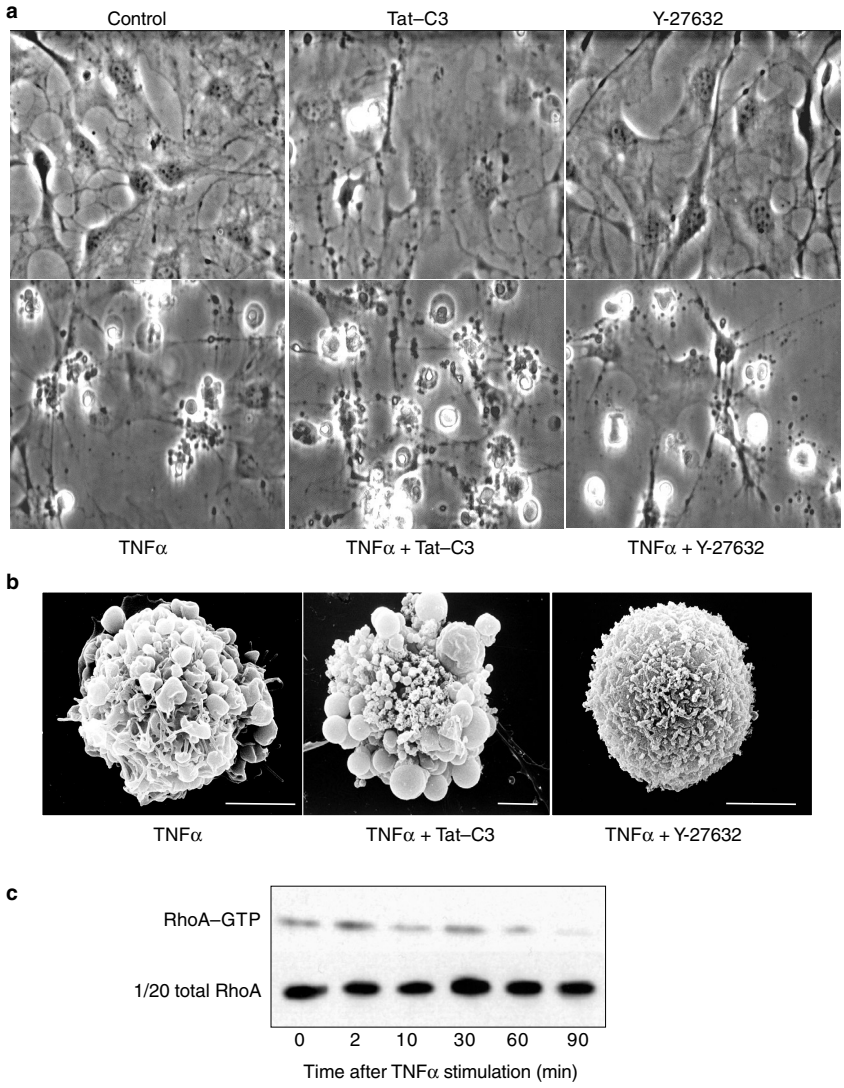

Figure 1 **Membrane blebbing during apoptosis is Rho-independent but ROCK-dependent. a**, Phase-contrast micrographs of NIH 3T3 mouse fibroblasts. Where indicated, cells were pretreated with 0.5 μM Tat–C3 for 18 h, treated with 25 ng ml^{-1} TNFα and 10 μg ml^{-1} cycloheximide for 2 h (TNFα), and/or treated with 10 μM Y-27632 for 2 h. **b**, Scanning electron micrographs of NIH 3T3 cells treated as in **a**. Scale bars represent 2.5 μm. **c**, Activation of RhoA by TNFα. Upper panel, RhoA–GTP pulled down by association with the Rho-binding domain of Rhotekin at the indicated times after TNFα stimulation; lower panel, 1/20 fraction of the total RhoA per lysate.

TNFα (Fig. 2b). Similar patterns of ROCK I cleavage were observed in Swiss 3T3 mouse fibroblasts and in MCF7 human breast carcinoma, MCF10A human breast epithelial and HA1 human embryonic kidney cells after treatment with TNFα and CHX (data not shown). The time course of ROCK I cleavage, which preceeded the generation of membrane blebs, paralleled that of PARP (Fig. 2b). Cleavage of both ROCK I and PARP was inhibited by pretreatment with the caspase inhibitor z-VAD-fmk (Fig. 2c).

Treatment with TNFα of NIH 3T3 cells transfected with a plasmid encoding human ROCK I with an N-terminal Myc tag, followed by western blotting with the anti-Myc monoclonal antibody 9E10 revealed that cleavage occurred ~200 amino acids from the C terminus of ROCK I (Fig. 3a and data not shown). Two potential sites of caspase cleavage, resembling the prototypical caspase-3 cleavage sequence DEVD, are situated in this region in both human and mouse ROCK I, at positions 1110–1113 (DETD) and 1155–1158 (DEQD), respectively. We changed these motifs to DETA (ROCK(D1113A)) and DEQA (ROCK(D1158A)), respectively, by site-directed mutagenesis and analysed them for cleavage by transfecting them into NIH 3T3 cells and then treating the cells with TNFα. Wild-type and D1158A ROCK I were cleaved to similar extents, whereas cleavage of ROCK(D1113A) was not detected (Fig. 3a). The cleaved forms of wild-type and D1158A ROCK I had the same apparent relative molecular weight as a mutant with an *opal* stop codon substituted for the glycine that is situated after the DETD (1110–1113) caspase-cleavage site (ROCK I(G1114*opa*)). As the C-terminal region of ROCK I has been reported to act as an auto-inhibitory domain[6,8–10], we compared the *in vitro* kinase activities of full-length wild-type ROCK I and the truncated G1,114*opa* mutant. Removal of the C-terminal 241 amino acids increased the phosphorylation of histone H1 by a factor of 7.8 ± 0.5 relative to the activity of full-length ROCK I (Fig. 3b). In addition, there was no detectable autophosphorylation of ROCK I(G1114*opa*), such as was observed for full-length ROCK I (Fig. 3b). Mutation to alanine

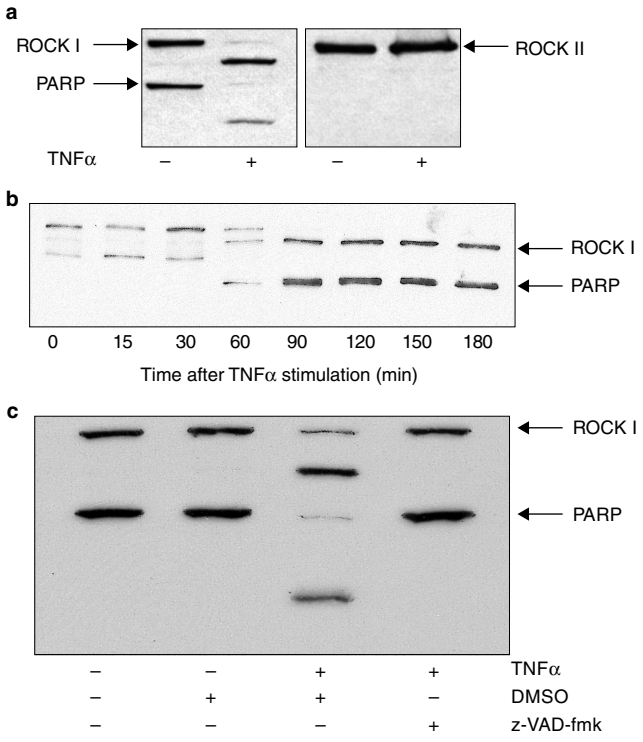

Figure 2 **ROCK I is a substrate for caspase-mediated proteolysis during TNFα-induced apoptosis. a**, Western blot of whole-cell lysates from untreated and TNFα-treated (3 h) NIH 3T3 cells, revealing proteolysis of ROCK I and PARP but not ROCK II. **b**, The time course of ROCK I cleavage parallels that of PARP cleavage. **c**, Cleavage of ROCK I and PARP is inhibited by pretreatment with 50 μM of the caspase inhibitor z-VAD-fmk for 2 h. Where indicated, dimethylsulphoxide (DMSO) was added.

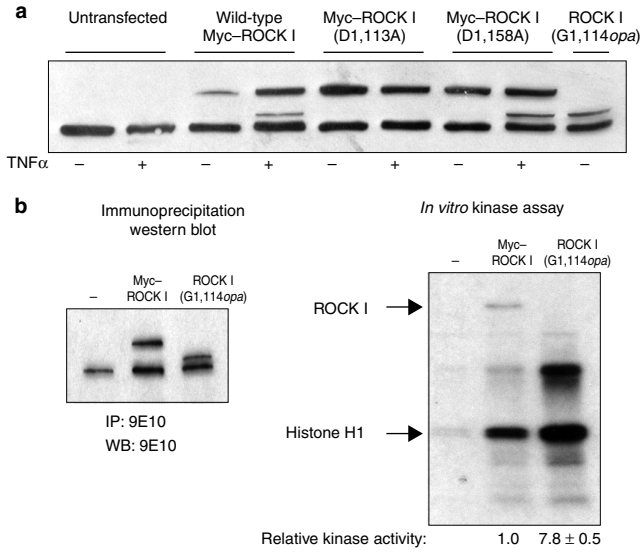

Figure 3 **Caspase-cleavage of ROCK I generates a truncated form with higher intrinsic kinase activity. a**, Transfection of NIH 3T3 cells with plasmids encoding wild-type and the indicated mutant constructs of human ROCK I, tagged with Myc at their N termini. Where indicated, cells were treated with TNFα for 3 h. **b**, NIH 3T3 cells were left untransfected (–) or were transfected with wild-type Myc-tagged ROCK I or a truncated G1114*opa* mutant. ROCK I was immunoprecipitated (IP) with the 9E10 monoclonal antibody and assayed for histone H1 kinase activity *in vitro* (right panel; see Methods). Autophosphorylated full-length ROCK I is indicated by an arrow. The efficiency of immunoprecipitation was determined by western blotting (WB) with 9E10 (left panel).

of the lysine residue that is critical for binding of ATP (K105A) abolished phosphorylation of histone H1 by immunoprecipitated full-length ROCK I and ROCK I(G1114*opa*) (data not shown). These results indicate that caspase activity during apoptosis leads to the removal of the C-terminal region of ROCK I and consequently to a release from the auto-inhibitory effect of this domain.

Active ROCK I is sufficient for cell contraction and dynamic membrane blebbing. To determine whether expression of truncated active ROCK I is sufficient to induce cell contraction and membrane blebbing similar to the morphological effects observed in response to TNFα treatment, we microinjected serum-starved NIH 3T3 cells either with a control plasmid encoding green fluorescent protein (GFP) alone (Fig. 4, left panels) or with plasmids encoding GFP plus ROCK I(G1114*opa*) (Fig. 4, right panels). Control GFP-expressing cells were indistinguishable from uninjected cells, with few actin stress fibres and little of the cell rising above 3 μm in height, as determined from serial *z*-sections obtained by confocal laser-scanning microscopy (Fig. 4a, b). In contrast, cells expressing ROCK I(G1114*opa*) contained thick parallel or, in some cases, 'stellate' actin stress fibres (Fig. 4a, right panels), as has been described for cells expressing constitutively activated forms of ROCK[6,9,24]. Cells expressing ROCK I(G1114*opa*) were contracted along the plane of the tissue-culture dish, and *z*-sections revealed that cell contraction was accompanied by formation of actin-containing blebs and increased cell height (Fig. 4a, b). These results indicate that active ROCK I(G1114*opa*) is sufficient to induce formation of thick stress fibres, thereby driving cell contraction which pushes the cell upwards.

To determine whether active ROCK I(G1114*opa*) can induce dynamic membrane blebbing independently of caspase activation, we treated serum-starved NIH 3T3 cells with 50 μM of the caspase inhibitor z-VAD-fmk for 1 h before microinjection. Two hours after co-microinjection with plasmids encoding GFP and ROCK I(G1114*opa*), we acquired time-lapse images of GFP-expressing cells by confocal microscopy. Figure 4c shows a representative cell with pronounced dynamic blebs that protrude and retract over a 25-min period. In fact, cells expressing ROCK I(G1114*opa*) blebbed over a period of several hours (data not shown), which contrasts with *bona fide* apoptotic blebbing, which lasts ~20–30 min in NIH 3T3 cells. These data support the conclusion that active ROCK I(G1114*opa*) is sufficient to promote formation of actin stress fibres and to drive cell contraction, resulting in dynamic membrane blebbing.

To determine whether the greater intrinsic kinase activity of the truncated form of ROCK I gives rise to a quantitative difference in cell contraction and blebbing relative to full-length ROCK I, we transfected NIH 3T3 cells with plasmids encoding Myc-tagged versions of ROCK I and ROCK I(G1114*opa*), or with a control plasmid encoding GFP. Overexpression of full-length ROCK I was sufficient to induce cell contraction and membrane blebbing in 25% of transfected cells, whereas ROCK I(G1114*opa*) induced the same morphological effects in 43% of transfected cells (Fig. 5a). Treatment of transfected cells with TNFα and CHX for a period of time that resulted in an apoptotic morphology in ~10% of GFP-expressing cells doubled the percentage of cells expressing full-length ROCK I that exhibited contraction and blebbing (Fig. 5a). In contrast, TNFα did not increase the percentage of cells expressing ROCK I(G1114*opa*) with blebs (Fig. 5a). These results indicate that ectopic expression of full-length ROCK I may increase the magnitude of the morphological response to TNFα by generating higher levels of cleaved active ROCK I, and that cells expressing ROCK I(G1114*opa*) may already have been fully responsive. This

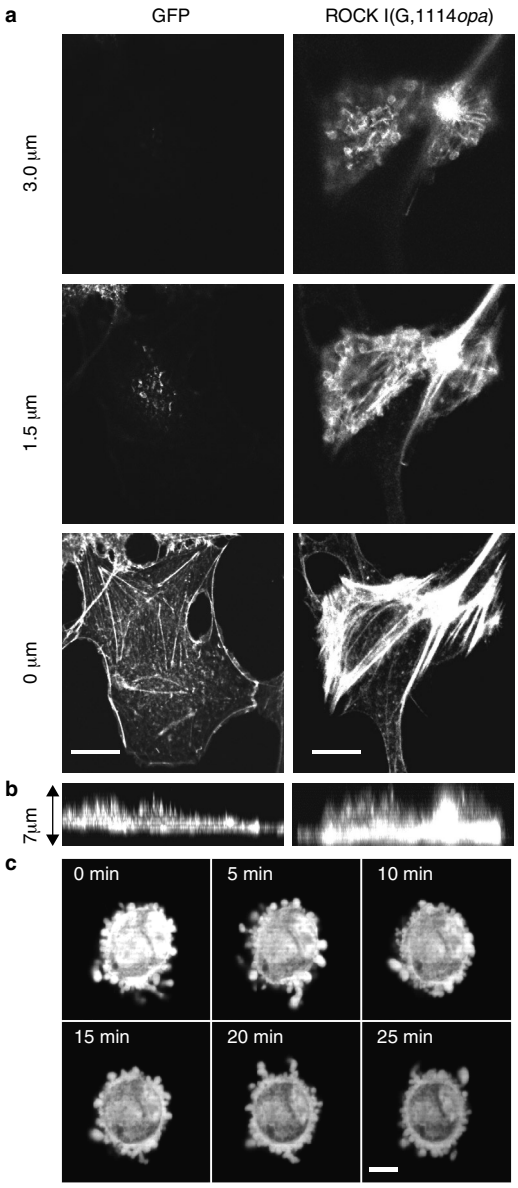

Figure 4 **Formation of actin stress fibres, cell contraction and dynamic membrane blebbing induced by active ROCK I. a**, Serum-starved NIH 3T3 cells were microinjected with plasmids encoding GFP or activated ROCK I(G1114*opa*). After 18 h, a *z*-series of images was acquired by confocal microscopy at intervals of 1.5 μm. Scale bar represents 10 μm. **b**, *z*-series images were acquired at intervals of 0.5 μm, compiled into a single view and then transposed from *x*–*y* views to *x*–*z* views. Height of image represents 7 μm in the *z*-dimension. **c**, Serum-starved NIH 3T3 fibroblasts were pretreated with 50 μM z-VAD-fmk for 1 h and then microinjected with plasmids encoding both GFP and truncated ROCK I(G1114*opa*). After 2 h, time-lapse images were obtained by confocal microscopy (see Supplementary Information). The first image is designated as time zero; subsequent images were obtained at the indicated times after. Scale bar represents 10 μm.

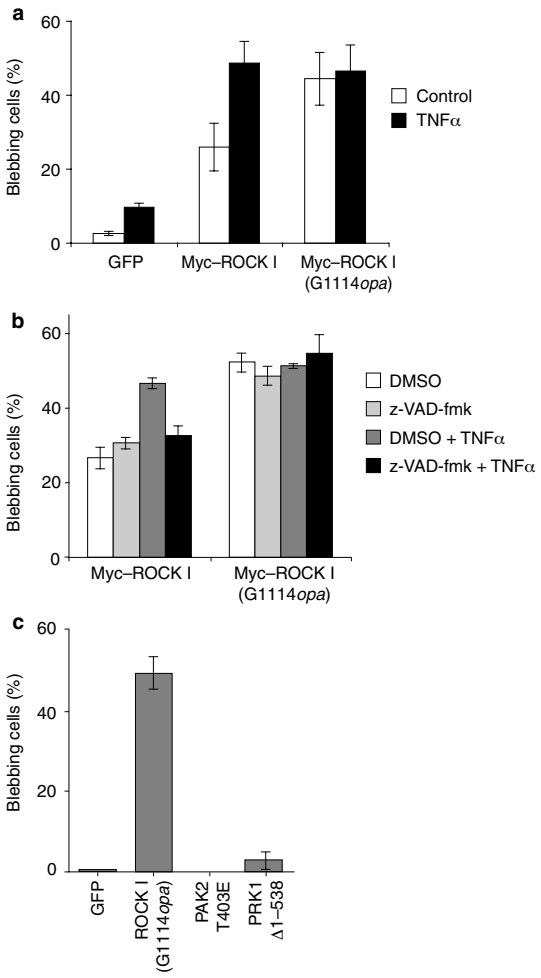

Figure 5 **Active ROCK I, but not active PAK2 or PRK1, promotes membrane blebbing in the presence of caspase inhibitor. a**, NIH 3T3 cells were transfected with plasmids encoding GFP, wild-type Myc–ROCK I or truncated Myc–ROCK I(G1114*opa*), and were either left untreated (open bars) or treated with 25 ng ml^{-1} TNFα and 10 μg ml^{-1} cycloheximide for 2 h (filled bars). After fixation and staining for ROCK I expression with 9E10 monoclonal antibody and for filamentous actin with phalloidin, the percentage of transfected cells exhibiting a contracted blebbing morphology was determined. Data are means ± s.e.m. from four determinations. **b**, NIH 3T3 cells were transfected with wild-type Myc–ROCK I or truncated Myc–ROCK I(G1114*opa*) and then treated as indicated (DMSO, dimethylsulphoxide). The percentage of transfected cells exhibiting blebbing morphology was determined; data are means ± s.e.m. from three determinations. **c**, The percentage of cells exhibiting blebbing morphology after microinjection of serum-starved NIH 3T3 cells with plasmids encoding GFP, ROCK I(G1114*opa*), PAK2 T403E and PRK1 Δ1–538 was determined; data are means ± s.e.m. from three determinations.

interpretation is supported by the fact that z-VAD-fmk did not affect the percentage of ROCK I(G1114*opa*)-expressing cells with a contracted blebbing morphology, but did block the TNFα-induced increase in blebbing in cells expressing full-length ROCK I (Fig. 5b).

Previous studies have shown that the Rho effector PRK1 (ref. 25) and the Rac and Cdc42 effector PAK2 (ref. 26) are cleaved during apoptosis to generate an active kinase fragment. We used active forms of PRK1 (ref. 27) and PAK2 (ref. 28) to determine whether, like active ROCK I(G1114*opa*), they are capable of generating cell contraction and membrane blebbing. As we observed in transfection experiments (Fig. 5a, b) microinjection of NIH 3T3 cells with active ROCK I(G1114*opa*) resulted in cell contraction and membrane blebbing in 50% of cells (Fig. 5c). The active PAK2(T403E) mutant[28] caused actin stress fibres to dissolve, and no microinjected cells showed signs of membrane blebbing or cell contractility. Consistent with previously published results[27], the N-terminally deleted active PRK1 had little effect on the actin cytoskeleton and did not significantly promote cell contractility or blebbing (Fig. 5c). These results support the idea that caspase-mediated cleavage and

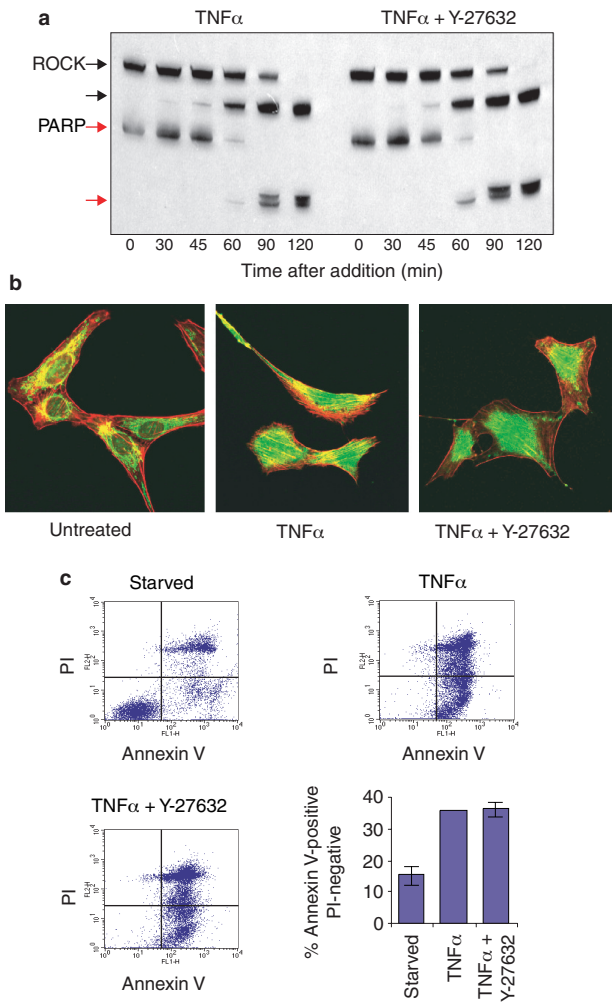

Figure 6 **ROCK activity is dispensable for caspase activation, cytochrome *c* release and phosphatidylserine externalization. a**, Y-27632 does not affect caspase cleavage of ROCK I and PARP. Serum-starved NIH 3T3 cells were treated with TNFα and CHX in the presence or absence of Y-27632 for the indicated times. Lysates were subjected to western blotting for ROCK I (black) and PARP (red). **b**, Y-27632 does not affect release of cytochrome *c* from mitochondria. Serum-starved NIH 3T3 cells were either left untreated or were treated with TNFα and CHX in the presence or absence of Y-27632 for 4 h. After fixation, cells were stained for cytochrome *c* (green) and filamentous actin (red). **c**, Y-27632 does not affect externalization of phosphatidylserine to the outer plasma membrane. Serum-starved NIH 3T3 cells were either left untreated (upper-left panel) or were treated with TNFα and CHX in the presence (lower-left panel) or absence (upper-right panel) of Y-27632 for 2.5 h. They were then stained for Annexin V binding and incorporation of propidium iodide (PI) and sorted by FACS. Normal cells are negative for both Annexin V and PI (lower-left quadrant), whereas apoptotic cells are positive for Annexin V and negative for PI (lower-right quadrant). Histogram (lower-right panel) shows the average percentage of Annexin V-positive, PI-negative cells for each treatment condition.

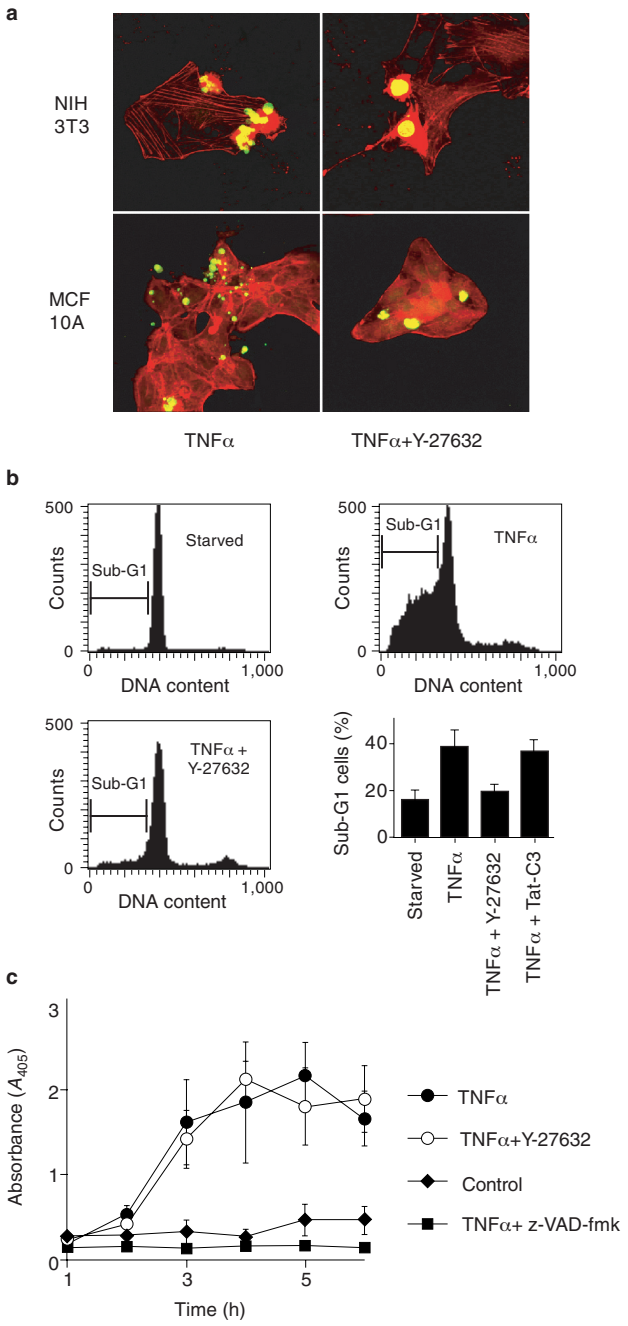

Figure 7 **ROCK-dependent membrane blebbing is required for localization of fragmented DNA to blebs and apoptotic bodies. a**, NIH 3T3 mouse fibroblasts and MCF10A human breast epithelial cells were treated with TNFα for 3 h or 20 h, respectively, in the presence or absence of 10 μM Y-27632. After fixation, fragmented DNA was stained by TUNEL using FITC-conjugated dUTP (green), and actin was stained with Texas Red–phalloidin (red). **b**, NIH 3T3 cells were serum-starved for 18 h (starved) and then treated for 3 h with TNFα, TNFα and Y-27632, or TNFα and Tat–C3 (Tat–C3 was included in the 18 h starvation medium) as indicated. Cells were collected and DNA content per cell (arbitrary units) was determined by staining with propidium iodide followed by FACS analysis. Apoptotic cells are defined as those with DNA content less than that typically present in G1 phase; data are means ± s.e.m. from four to eight determinations per treatment. **c**, The time course of DNA fragmentation was determined in quadruplicate by monitoring histone-associated DNA fragments using an ELISA of serum-starved NIH 3T3 cells that were either left untreated (control) or treated with TNFα, TNFα and Y-27632, or TNFα and z-VAD-fmk.

subsequent activation of ROCK I are key events in the generation of the morphological changes that occur during apoptosis.

ROCK activity is necessary for relocalization of fragmented DNA. By administering Y-27632 together with TNFα and CHX, we determined that ROCK does not function in the biochemical processes of apoptosis, including caspase-mediated cleavage of ROCK I and PARP (Fig. 6a), release of cytochrome *c* from mitochondria (Fig. 6b), and presentation of phosphatidylserine on the outer plasma

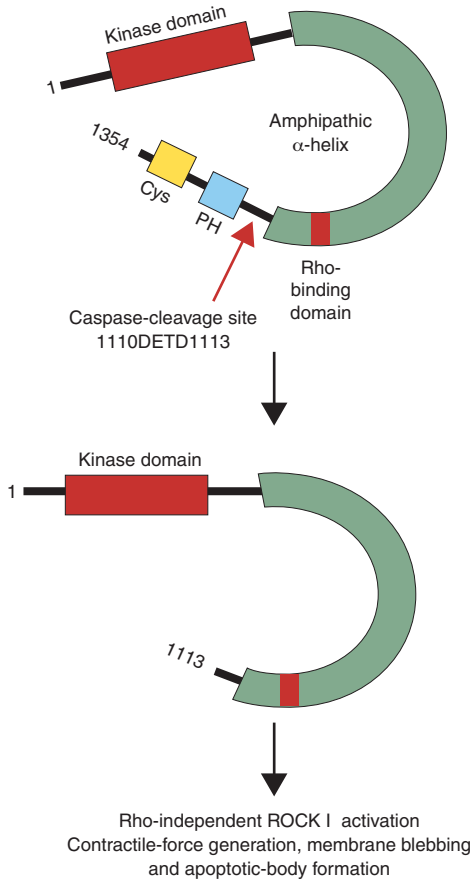

Figure 8 **Caspase-mediated cleavage of ROCK I during apoptosis leads to loss of its auto-inhibitory domain.** ROCK I phosphorylation of substrates results in generation of contractile force, which drives formation of membrane blebs and apoptotic bodies. PH, pleckstrin-homology domain; Cys, cysteine-rich domain.

membrane (Fig. 6c). However, staining of fragmented DNA *in situ* by TdT-mediated dUTP nick-end labelling (TUNEL) in TNFα-treated NIH 3T3 cells showed that fragmented DNA was localized within membrane blebs, and in MCF10A cells fragmented DNA was found in blebs and apoptotic bodies (Fig. 7a). In contrast, fragmented DNA in cells treated with TNFα and Y-27632 was localized in single, discrete focal points within each cell (Fig. 7a). These changes in the localization of fragmented DNA also resulted in differences in DNA content per cell, as determined by staining with propidium iodide and fluorescence-activated cell sorting (FACS). The proportion of serum-starved cells with a DNA content less than that which is typically present in G1 phase rose from 15% to 40% after treatment with TNFα and CHX, although supplementing with Y-27632 kept the proportion of such 'sub-G1' cells at 18% (Fig. 7b). Pretreatment with Tat–C3 did not affect the proportion of sub-G1 cells observed after TNFα treatment (Fig. 7b). The reduction in the percentage of sub-G1 after Y-27632 treatment did not result from reduced DNA fragmentation, as determined using an enzyme-linked immunosorbent assay (ELISA) against histone-associated DNA fragments (Fig. 7c) or by direct examination of DNA from detergent-lysed cells by gel electrophoresis (data not shown). By inhibiting membrane blebbing, Y-27632 reduced the relocalization of fragmented DNA from the central nuclear region into apoptotic bodies, resulting in a reduction in the loss of DNA from apoptotic bodies either before or during fixation and staining for FACS analysis[29].

Discussion

In a normal cellular context, ROCK is activated by Rho–GTP, which probably shifts the C-terminal auto-inhibitory domain away from the kinase active site by inducing a conformational change and/or by promoting autophosphorylation within this region. In cooperation with other Rho-effector proteins, particularly mDia, ROCK proteins contribute to agonist-induced changes to the actin cytoskeleton without necessarily producing marked contraction and blebbing[30,31]. During apoptosis, caspase-mediated cleavage after the DETD (1110–1113) sequence removes the putative autophosphorylation/auto-inhibitory domain, leading to Rho-independent activation of ROCK I (Fig. 8). Through phosphorylation of downstream targets, active caspase-cleaved ROCK I promotes generation of actin–myosin force, cell contractility and consequent membrane blebbing and formation of apoptotic bodies.

By treating apoptotic cells with the ROCK inhibitor Y-27632, we determined that caspase-mediated activation of this kinase and, by inference, membrane blebbing, do not contribute to the biochemical events that occur as part of the apoptotic programme. Caspase activation, DNA fragmentation and release of cytochrome *c* from mitochondrial stores were all unaffected by Y-27632. In addition, despite the inhibition of blebbing, externalization of phosphatidylserine proceeded normally in Y-27632-treated apoptotic cells. These results indicate that the gross morphological changes that accompany apoptotic membrane blebbing do not contribute significantly to the process of phosphatidylserine display on the outer plasma membrane. Although non-blebbing apoptotic cells appeared to exhibit the same biochemical characteristics as blebbing cells, it remains to be seen whether inhibition of blebbing would affect processes that are associated with apoptosis *in vivo*, such as recognition and clearance of the apoptotic cell by the immune system.

The most notable consequence that resulted from repression of blebbing was that fragmented DNA was no longer relocalized from the nuclear region into blebs and apoptotic bodies. These results indicate that the same dynamic forces that drive protrusions from the plasma membrane during apoptosis may be responsible for destruction of the nuclear envelope and laminar matrix. Future experiments will reveal whether caspase-mediated degradation of integral membrane proteins, nuclear lamins and lamin-associated proteins is sufficient to disrupt the integrity of nuclear membranes, or whether rearrangement of the actin cytoskeleton during apoptosis is also required. □

Methods

Cell culture, transfection and western blotting.

NIH 3T3 cells were grown in DMEM supplemented with 10% donor calf serum and were placed in serum-free medium 18 h before treatment with 25 ng ml^{-1} recombinant mouse TNFα (R&D Systems, Abingdon, UK) plus 10 μg ml^{-1} cycloheximide (Sigma). Transfections were carried out as described[32]. Cells were scraped and collected in their media, centrifuged at 7,000*g* for 20 min and lysed in buffer containing 10 mM Tris pH 7.5, 5 mM EDTA, 150 mM NaCl, 40 mM sodium pyrophosphate, 1 mM Na_3VO_4, 50 mM NaF, 1% (*v*/*v*)NP-40, 0.5% (*w*/*v*)sodium deoxycholate, 0.025% (*w*/*v*)SDS and 1 mM *p*-aminoethy-benzene sulphonyl fluoride. Supernatants were clarified by centrifugation at 13,000*g* for 15 min and 100 μg of cell lysate were run on 10% SDS–polyacrylamide gels, transferred to nitrocellulose membranes and blocked in TBS containing 5% (*w*/*v*)dried milk before western blotting with anti-ROCK II (Transduction Laboratories), anti-ROCK I (Transduction Laboratories) or anti-PARP (PharMingen) antibodies.

Plasmids.

Mammalian expression vector pCAG-Myc–ROCK I (a gift from S. Narumiya, Kyoto Univ., Japan) is described elsewhere[8]. Amino-acid substitutions were introduced using a QuikChange Site-Directed Mutagenesis Kit (Stratagene) according to the manufacturer's instructions. Expression plamids pCAN-Myc–PAK2 T403E (ref. 28) and pEF-Myc–PRK1 Δ1–538 (ref. 27) are described elsewhere.

ROCK I kinase assays.

Myc-tagged ROCK I was immunoprecipitated from whole-cell lysates with 5 μg of 9E10 mouse monoclonal antibody per sample and protein G–sepharose (Pharmacia). Immunoprecipitates were washed three times in buffer containing 50 mM Tris pH 7.5, 10 mM $MgCl_2$, 0.1 mM *p*-aminoethy-benzene sulphonyl fluoride, 40 mM sodium pyrophosphate, 1 mM Na_3VO_4, 50 mM NaCl, 1 mM dithiothreitol (DTT), 10% glycerol and 0.03% Brij 35, washed twice in kinase-assay buffer containing 50 mM Tris pH 7.5, 1 mM EDTA, 10 mM $MgCl_2$, 50 mM NaCl, 1 mM DTT and 0.03% Brij 35, and finally resus-

pended in 30 µl of kinase-assay buffer containing 10 µM ATP, 50 ng µl^{-1} histone H1 and 135 nCi µl^{-1} [^{32}P]ATP. Samples were incubated for 30 min at 30 °C, terminated by addition of Laemmli buffer, run on 10% SDS–polyacrylamide gels and then transferred to nitrocellulose membranes. Relative kinase activity was quantified using a Molecular Dynamics Storm Phosphoimager and data are expressed as means ± s.e.m. from five experiments.

Scanning electron microscopy.

NIH 3T3 cells were treated as indicated for 3 h, fixed in 2% glutaraldehyde (electron-microscopy grade, Sigma), treated with osmium tetroxide in sodium cacodylate buffer, dehydrated with sequential washes in 70%, 90% and 100% ethanol, and then dried with hexamethyldisilazane (Sigma) before coating with gold.

Rho pull-down assay.

Cells (5 × 10^5) were plated in 10-cm dishes, serum-starved after 48 h and lysed 24 h after serum starvation in 50 mM Tris pH 7.2, 500 mM NaCl, 1% (*v*/*v*)Triton X-100, 5 mM $MgCl_2$, 1 mM DTT and protease inhibitors. Cell lysates (30 µl) were subjected to western blotting; the remainder was spun at 10,000*g* for 5 min. The supernatant was then mixed with ~10 µg of bacterially expressed GST–Rhotekin (murine amino acids 7–89) bound to glutathione–sepharose and was incubated at 4 °C with tumbling for 30 min. Samples were briefly spun, the supernatant was removed and beads were washed twice in 50 mM Tris pH 7.2, 150 mM NaCl, 1% (*v*/*v*)Triton X-100, 5 mM $MgCl_2$ and 1 mM DTT before addition of Laemmli buffer and analysis by western blotting with anti-RhoA antibody (Santa Cruz).

Recombinant proteins and cell-permeable C3.

pGEX-KG C3 (a gift from R. Treisman, ICRF, London) was modified to include the nucleotide sequence 5′-GGAGGATACGGCCGAAAGAAGCGACGACAGCGACGCCGTGGAGGA of the thrombin cleavage site at a position 5′ to the C3-encoding sequence. Recombinant proteins were produced in *E. coli* BL21 carrying *plysS*; protein expression was induced in 1-l cultures with 0.3 mM isopropyl-β-thio-galactopyranoside (IPTG) for 3 h at 32 °C. Cells were lysed in TBS with 5 mM $MgCl_2$, 1 mM DTT and protease inhibitors by rapid freezing followed by sonication. After centrifugation at 10,000*g* for 10 min at 4 °C the supernatant was incubated with glutathione–sepharose for 2 h at 4 °C and beads were extensively washed with TBS plus 5 mM $MgCl_2$ and 1 mM DTT. To cleave Tat–C3, beads were incubated in TBS plus 1 mM $MgCl_2$, 1 mM $CaCl_2$, 1 mM DTT and 30 units of thrombin overnight at 4 °C; the supernatant was then removed and incubated with *p*-aminobenzamidine beads for 1 h. Supernatant containing Tat–C3 was then snap-frozen and used at 0.5 µM in cell-culture media.

Microinjection and immunofluorescence.

Serum-starved NIH 3T3 cells were microinjected with plasmids encoding ROCK I(G1,114*opa*), PAK2 T403E or PRK1 Δ1–538 at a concentration of 100 ng µl^{-1}; plasmids encoding GFP were microinjected at 25 ng µl^{-1}, and 12 h were allowed for protein expression. Cells were fixed and stained for filamentous actin structures as described[27]. For visualization of cytochrome *c*, cells were treated as indicated for 4 h, after which they were fixed and stained with anti-cytochrome *c* monoclonal antibody (PharMingen) at 1:500 dilution and then with fluorescein isothiocyante (FITC)-conjugated donkey anti-mouse antibody (Jackson Laboratories)at 1:250 dilution and Texas Red-conjugated phalloidin (Molecular Probes)at 0.5 µg ml^{-1}. Confocal laser-scanning microscopy was carried out using a Bio-Rad MRC 1024 microscope.

DNA-fragmentation ELISA.

Histone-associated DNA fragments were detected using the Cell Death Detection ELISA kit (Roche). Lysates from 10^3 cells for each of the indicated time points were processed according to the manufacturer's instructions and absorbance at 405 nm was determined.

Detection of phosphatidylserine externalization by FACS analysis.

Serum-starved NIH 3T3 were treated with TNFα, CHX and, where indicated, 10 µM Y-27632 for 2.5 h. Cells were detached by trypsinization and were then centrifuged, washed in ice-cold PBS and suspended in Annexin V binding buffer (10 mM HEPES, 140 mM NaCl and 2.5 mM $CaCl_2$, pH 7.4) to a final density of 1 × 10^6 cells per ml. To 1 × 10^5 cells were added 5 µl of FITC-conjugated Annexin V (Pharmingen) and 2 µl of 50 µg ml^{-1} propidium iodide. After incubation at room temperature for 15 min, 400 µl binding buffer was added and Annexin V binding was analysed using a Becton Dickinson FACSCalibur.

FACS analysis of DNA content.

NIH 3T3 cells were serum-starved for 18 h and were then treated with TNFα and CHX for 3 h, detached by trypsinization, centrifuged and fixed in cold 70% ethanol for 15 min at –20 °C. After centrifugation, cells were resuspended in PBS containing 40 µg ml^{-1} propidium iodide and 300 µg ml^{-1} RNase A, then incubated at 37 °C for 30 min before analysis using a Becton Dickinson FACSCalibur.

RECEIVED 4 OCTOBER 2000; REVISED 24 NOVEMBER 2000; ACCEPTED 24 NOVEMBER 2000; PUBLISHED 6 MARCH 2001.

1. Cotter, T. G., Lennon, S. V., Glynn, J. M. & Green, D. R. Microfilament-disrupting agents prevent the formation of apoptotic bodies in tumor cells undergoing apoptosis. *Cancer Res.* **52,** 997–1005 (1992).
2. Mills, J. C., Stone, N. L., Erhardt, J. & Pittman, R. N. Apoptotic membrane blebbing is regulated by myosin light chain phosphorylation. *J. Cell Biol.* **140,** 627–636 (1998).
3. Torgerson, R. R. & McNiven, M. A. The actin-myosin cytoskeleton mediates reversible agonist-induced membrane blebbing. *J. Cell Sci.* **111,** 2911–2922 (1998).
4. Hall, A. Rho GTPases and the actin cytoskeleton. *Science* **279,** 509–514 (1998).
5. Matsui, T. *et al.* Rho-associated kinase, a novel serine/threonine kinase, as a putative target for small GTP binding protein Rho. *EMBO J.* **15,** 2208–2216 (1996).
6. Leung, T., Chen, X. Q., Manser, E. & Lim, L. The p160 RhoA-binding kinase ROK alpha is a member of a kinase family and is involved in the reorganization of the cytoskeleton. *Mol. Cell. Biol.* **16,** 5313–5327 (1996).
7. Ishizaki, T. *et al.* The small GTP-binding protein Rho binds to and activates a 160 kDa Ser/Thr protein kinase homologous to myotonic dystrophy kinase. *EMBO J.* **15,** 1885–1893 (1996).
8. Ishizaki, T. *et al.* p160ROCK, a Rho-associated coiled-coil forming protein kinase, works downstream of Rho and induces focal adhesions. *FEBS Lett.* **404,** 118–124 (1997).
9. Amano, M. *et al.* Formation of actin stress fibers and focal adhesions enhanced by Rho-kinase. *Science* **275,** 1308–1311 (1997).
10. Amano, M. *et al.* The COOH terminus of Rho-kinase negatively regulates rho-kinase activity. *J. Biol. Chem.* **274,** 32418–32424 (1999).
11. Amano, M. *et al.* Phosphorylation and activation of myosin by Rho-associated kinase (Rho-kinase). *J. Biol. Chem.* **271,** 20246–20249 (1996).
12. Matsui, T. *et al.* Rho-kinase phosphorylates COOH-terminal threonines of ezrin/radixin/moesin (ERM) proteins and regulates their head-to-tail association. *J. Cell. Biol.* **140,** 647–657 (1998).
13. Kimura, K. *et al.* Regulation of myosin phosphatase by Rho and Rho-associated kinase (Rho-kinase). *Science* **273,** 245–248 (1996).
14. Kureishi, Y. *et al.* Rho-associated kinase directly induces smooth muscle contraction through myosin light chain phosphorylation. *J. Biol. Chem.* **272,** 12257–12260 (1997).
15. Kaneko, T. *et al.* Identification of calponin as a novel substrate of Rho-kinase. *Biochem. Biophys. Res. Commun.* **273,** 110–116 (2000).
16. Koyama, M. *et al.* Phosphorylation of CPI-17, an inhibitory phosphoprotein of smooth muscle myosin phosphatase, by Rho-kinase. *FEBS Lett.* **475,** 197–200 (2000).
17. Maekawa, M. *et al.* Signaling from Rho to the actin cytoskeleton through protein kinases ROCK and LIM-kinase. *Science* **285,** 895–898 (1999).
18. Aktories, K., Mohr, C. & Koch, G. Clostridium botulinum C3 ADP-ribosyltransferase. *Curr. Top. Microbiol. Immunol.* **175,** 115–131 (1992).
19. Uehata, M. *et al.* Calcium sensitization of smooth muscle mediated by a Rho-associated protein kinase in hypertension. *Nature* **389,** 990–994 (1997).
20. Reid, T. *et al.* Rhotekin, a new putative target for Rho bearing homology to a serine/threonine kinase, PKN, and rhophilin in the rho-binding domain. *J. Biol. Chem.* **271,** 13556–13560 (1996).
21. Ren, X. D., Kiosses, W. B. & Schwartz, M. A. Regulation of the small GTP-binding protein Rho by cell adhesion and the cytoskeleton. *EMBO J.* **18,** 578–585 (1999).
22. Earnshaw, W. C., Martins, L. M. & Kaufmann, S. H. Mammalian caspases: structure, activation, substrates, and functions during apoptosis. *Annu. Rev. Biochem.* **68,** 383–424 (1999).
23. Bokoch, G. M. Caspase-mediated activation of PAK2 during apoptosis: proteolytic kinase activation as a general mechanism of apoptotic signal transduction? *Cell Death Differ.* **5,** 637–645 (1998).
24. Nakano, K. *et al.* Distinct actions and cooperative roles of ROCK and mDia in Rho small G protein-induced reorganization of the actin cytoskeleton in Madin–Darby canine kidney cells. *Mol. Biol. Cell* **10,** 2481–2491 (1999).
25. Takahashi, M., Mukai, H., Toshimori, M., Miyamoto, M. & Ono, Y. Proteolytic activation of PKN by caspase-3 or related protease during apoptosis. *Proc. Natl Acad. Sci. USA* **95,** 11566–11571 (1998).
26. Rudel, T. & Bokoch, G. M. Membrane and morphological changes in apoptotic cells regulated by caspase-mediated activation of PAK2. *Science* **276,** 1571–1574 (1997).
27. Sahai, E., Alberts, A. S. & Treisman, R. RhoA effector mutants reveal distinct effector pathways for cytoskeletal reorganization, SRF activation and transformation. *EMBO J.* **17,** 1350–1361 (1998).
28. Zeng, Q. *et al.* Endothelial cell retraction is induced by PAK2 monophosphorylation of myosin II. *J. Cell Sci.* **113,** 471–482 (2000).
29. Darzynkiewicz, Z. *et al.* Features of apoptotic cells measured by flow cytometry. *Cytometry* **13,** 795–808 (1992).
30. Watanabe, N., Kato, T., Fujita, A., Ishizaki, T. & Narumiya, S. Cooperation between mDia1 and ROCK in Rho-induced actin reorganization. *Nature Cell Biol.* **1,** 136–143 (1999).
31. Tominaga, T. *et al.* Diaphanous-related formins bridge Rho GTPase and Src tyrosine kinase signaling. *Mol. Cell* **5,** 13–25 (2000).
32. Marais, R., Light, Y., Paterson, H. F. & Marshall, C. J. Ras recruits Raf-1 to the plasma membrane for activation by tyrosine phosphorylation. *EMBO J.* **14,** 3136–3145 (1995).

ACKNOWLEDGEMENTS

We thank R. Marais and C. Marshall for discussions, H. Patterson, A. Tutt, D. Robertson and I. Titley for technical advice, J. Riedl for recombinant Tat–C3 protein, the Welfide Corporation for Y-27632, R. Treisman for pGEX-KG C3, A. Ridley for pCAN-PAK2 (T403E), and S. Narumiya for pCAG-Myc–ROCK I. This work was supported by a project grant from the Cancer Research Campaign. M.F.O. is a Mr and Mrs John Jaffe Donation University Research Fellow of The Royal Society.
Correspondence and requests for materials should be addressed to M.F.O. Supplementary Information is available on *Nature Cell Biology*'s website (http://cellbio.nature.com).

Movie 1 **Cell contraction and dynamic membrane blebbing induced by active ROCK I.** Serum-starved NIH 3T3 fibroblasts were pretreated with 50 μM z-VAD-fmk for 1 h and then microinjected with plasmids encoding both GFP and truncated ROCK I(G1,114*opa*). After 2 h, time-lapse images were obtained by visualizing expressed GFP using confocal microscopy over a period of 25 min.